



Shahrood University of
Technology



Iranian Society of
Mining Engineering
(IRSM)

Application of machine learning algorithms for prediction of Blast-induced Ground Vibration in View of Stiffness Ratio, Energy Coverage and Scaled Distance

Yasar Agan*, and Turker Hudaverdi

Department of Mining Engineering, Istanbul Technical University, Istanbul, Türkiye

Article Info

Received 31 January 2025

Received in Revised form 22 April 2025

Accepted 16 May 2025

Published online 16 May 2025

DOI: [10.22044/jme.2025.15686.3016](https://doi.org/10.22044/jme.2025.15686.3016)

Keywords

Adaptive-network-based fuzzy inference system (ANFIS)

Blasting

Gaussian process regression (GPR)

Ground vibration

Support vector machine (SVM)

Abstract

The purpose of this research work is to predict blast induced ground vibration in surface mine by using classical and machine learning algorithms. For the purpose of minimizing blast-induced ground vibration to acceptable levels, the level of vibration must be predicted. Blast-induced ground vibration is defined peak particle velocity (ppv) in the ground. All data used to estimation were obtained by observing real blasting operations. After the measuring of the peak particle velocity, models of the prediction were created using independent site parameters. Most of the data is used to train the model, while remaining part is used for testing. The models were created using independent blasting parameters proportionally. Thus, more parameters are included in the models without complicating the models. A thorough validation process was conducted utilizing a diverse set of nine error criteria. Artificial intelligence models have been found to outperform traditional methods in predicting ground vibration. The mean absolute error values were found to be 1.42, 1.54, and 1.78 for ANFIS, GPR, and SVM, respectively. A similar situation is observed for other error criteria as well. ANFIS appears to be the most effective model for predicting ground vibration.

1. Introduction

In an open mine, optimum rock fragmentation should be achieved with minimum cost. Bench blasting is the main method for rock excavation. Performance of blasting operation may be discussed considering different factors. Engineers try to obtain a suitable particle size distribution. Size distribution affects all the downstream processes. Movement and shape of the muckpile also influence overall productivity. Machines cannot load a tight muckpile easily. Large muckpile means a large clean-up area. Excavators and dozers work excessively. On the other hand, a too high muckpile may create danger for the excavators. In addition, back break and side break should also be considered. Blasting should be performed without disturbing surrounding rock. Some special blasting

techniques may be applied to reduce back break such as smooth blasting and pre-splitting [1, 2].

Blasting has also many environmental adverse effects including ground vibration, flyrock, air blast and dust. Blast-induced environmental effects should be reduced as much as possible to perform a sustainable excavation operation. Especially, blast-induced ground vibration is a significant concern. Vibration waves may reach far distances. If ground vibration is higher than an acceptable level, it can cause damage to surrounding infrastructure. Some precautions may be considered, such as reduction of explosive charge per hole or increase of delay between blastholes.

Several site variables are effective in blast induced environmental effects. These variables can be categorized into two group as controllable and



uncontrollable parameters. The controllable parameters (blast design parameters) are spacing, burden, bench height, stemming, sub-drilling, spacing between holes, and drillhole diameter. These parameters can be adjusted by engineers considering site conditions. Uncontrollable parameters are mechanical and physical properties of rock and rock mass structure. Prediction of ground vibrations provides great advantages for site engineers. Classical scaled distance-based equations have been widely used in blasting literature [3]. Kahrman [4] used square root scaled distance approach to predict peak particle velocity (ppv) in a limestone quarry. Ataei [5] applied conventional predictors to forecast ground vibrations during Karoun 3 power plant and dam excavations. Yılmaz [6] and Hudaverdi and Akyıldız [7] compared most widely used ground vibration predictor equations. In last decade, machine learning algorithms have also been practiced for ground vibration estimation. Mohammadi et al. [8] used the adaptive neuro fuzzy inference system (ANFIS) technique to predict particle velocity for ANFO and emulsion-type explosives. Kamali and Ataei [9, 10] and Armaghani et al. [11] also applied feed forward-back propagation neural networks and ANFIS method. Akyıldız and Hudaverdi [12] used the ANFIS algorithms to estimate blast-induced ground vibrations considering stiffness ratio. Hasanipanah et al. [13] and Dindarloo [14] practiced support vector machines (SVM). Some researchers applied gene expression programming (GEP) and genetic algorithms to create robust predictive models [15, 16, 17].

In recent years, some new algorithms have become popular. Mohammadi et al. [18] tested a combination of the imperialist competitive algorithm (ICA) and k-means algorithm to cluster the measured data. Komadja et al [19] applied multivariate adaptive regression splines (MARS) in addition to classification and regression tree (CART) and SVM. Nguyen et al. [20] investigated efficiency of self-organizing neural networks (SONIA) using different metaheuristic algorithms. Chandrahas et al. [21] applied XG boost algorithm to predict both rock fragmentation and ground vibration. According to blast literature, blast design parameters are generally most dominant parameters in creating prediction models.

In this study, ANFIS, SVM and gaussian process regression (GPR) techniques were used to predict blast-induced vibrations. Generally, method selection is performed randomly. However, in this research, there was a specific consideration during

method selection process. Each selected method relies on a different concept. ANFIS is a neural network rooted Takagi-Sugeno fuzzy system, integrating both artificial neural networks and fuzzy logic concepts. It seeks to establish fuzzy IF-THEN rules using a single output value. ANFIS employs a hybrid learning technique that integrates the least squares method with backpropagation gradient descent techniques [22]. SVM is a supervised machine learning strategy derived from statistical learning theory [23]. SVM utilize a kernel function-based nonlinear mapping to project an input space into a multidimensional space. Then, it identifies a nonlinear relationship between inputs and outputs within this space [24]. Gaussian process regression is a type of Bayesian non-parametrical technique that effectively manages data uncertainties in a systematic way. GPR is a stochastic process [25].

In addition, the blast design parameters were also not chosen randomly. Stiffness ratio (Bench height/Burden, H/B), spacing/burden ratio (S/B) and scaled distance (SD) were selected as input parameters. Stiffness ratio (H/B) expresses the ratio of bench height to burden and varies between 1 and 4. It directly affects vibration intensity and fragmentation efficiency. According to Konya and Walter [2], if H/B is lower than 2, ground vibration levels increases and problems such as backbreak, hard toe and coarse fragmentation may occur. On the other hand, if H/B ratio is around 3, the ground vibration levels decrease and successful fragmentation is achieved [2]. The S/B ratio is referred as energy coverage in the literature. Olofsson [26] indicates that S/B ratio highly influences fragment size. If the S/B ratio is greater than 1.25, fine-grained fragmentation can be obtained. If S/B is less than 1.25, coarse-grained fragmentation is obtained and energy may be lost as ground vibration. The last input parameter selected is the scaled distance. SD represents the proportion of the vibration measurement distance (D) to maximum charge weight per delay (W). Scaled distance concept is a fundamental parameter especially for predictive equations [26].

The developed machine learning models were evaluated against the traditional predictive formulas derived from regression analysis. Model comparison, which is usually made according to one or two error criteria in the literature, was performed using eight different error criteria in this study. ANFIS model was found to be superior to other models considering some specific error criteria. SVM and GPR models also provided satisfactory results. In general, machine learning

methods have predicted ground vibration much more successfully than classical prediction techniques.

In the following pages, firstly, the field measurements are initially detailed. The third section covers traditional prediction formulas. The equations based on scaled distance and the multiple regression equation are presented. The following section discusses development of machine learning models. ANFIS, GPR and SVM models were explained in detail. Section six discusses the model testing stage. The regression equations were compared to machine learning models using

different accuracy measures. The last part evaluates general findings of the research.

2. Field Measurements

All the site data were collected at Akdaglar sandstone quarry in Northern Istanbul, Kemerburgaz region. There are five neighboring quarries in the region. The satellite image of the mine site is shown in Figure 1 [27]. The quarries are very close to human settlements. There are hospitals, factories and highways in the close proximity of quarries.

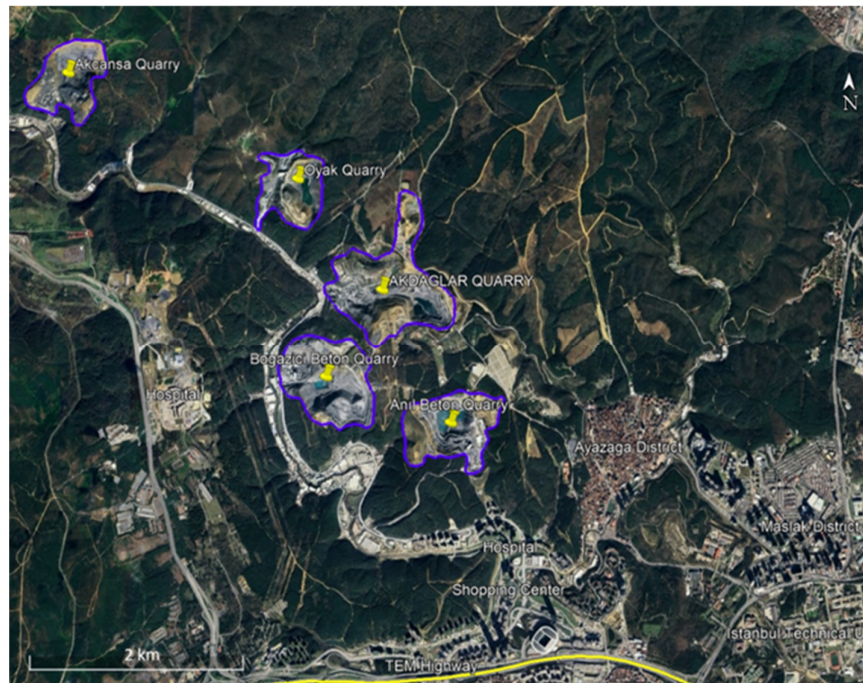


Figure 1. Satellite image of the mining site and surrounding settlements

The blasted rock material is processed by crushing and screening plants with a capacity of 1100 tons/h to produce the aggregate required for asphalt and concrete plants. The production capacity is 6 million tons per year. The mine is situated in the Trakya region (west of the Bosphorus), and the primary geological formation found there is the Lower Carboniferous Trakya formation. The Trakya formation predominantly comprises siltstone, shale, and sandstone metamorphisms. There are limestone layers of various thicknesses in the lower parts and conglomerate lenses in its middle and upper parts [28]. The thickness of sandstone layers varies between 50 cm and 100 cm. Andesite and diabase intrusions are also observed in some regions.

ANFO is used as the main explosive in the studied quarry and it is charged into 89 mm

drillholes. The drilling pattern is staggered and the initiation was carried out using non-electric detonators. A total of 95 vibration measurement data were taken to build vibration forecasting models. The average spacing distance in the quarry, with a standard deviation of 0.38 m, is 2.74 m. The average burden, with a standard deviation of 0.37 m, is 2.30 m. Mean bench height is 7.56 m. The distance between blast locations and observation points was quantified with two different handheld GPS devices. Vibration data were recorded by InstanTel Micromate blast seismographs. The seismograph is capable of measuring particle velocities between 0.127 and 254 mm/s. The statistical data of the site measurements are shown in the Table 1.

Table 1. Descriptive statistics for the blast design parameters and vibration measurement

Parameters	Min	Max	Range	Average	Std Deviation
S (m)	2.13	5.00	2.87	2.74	0.378
B (m)	1.49	4.00	2.51	2.30	0.371
T (m)	1.80	6.00	4.20	2.85	0.907
H (m)	3.50	14.00	10.5	7.56	2.025
S/B (m)	0.75	1.66	0.91	1.019	0.162
H/B (m)	1.31	5.88	4.58	3.34	0.993
D (m)	27	400	373	137.18	72.162
W (kg)	14.92	279.81	264.89	68.73	48.509
SD (m/kg ^{0.5})	1.85	35.12	33.26	17.51	6.886
ppv (mm/s)	1.72	32.79	31.07	7.17	5.647

S: Spacing, B: Burden, T: Stemming, H: Bench of height, W: Instantaneous explosive charge, D: Vibration monitoring distance, SD: Scaled distance, ppv: Measured peak particle velocity, Monitored blast no (n): 95.

3. Classical Predictor Equations for Ground Vibration

3.1 Scaled distance-based equations

The pioneering effort to develop a ground vibration model was carried out by the U.S Bureau of Mines (USBM) and Crandell. According to USBM model, magnitude of particle velocity is mainly affected by two factors; the maximum instantaneous charge per delay and the interval between blasting site and vibration measuring point [29]. The scaled distance is calculated by using the ratio of the distance to the charge weight. Today, USBM model is one of the most referred scaled distance approaches [30]:

$$SD = \frac{D}{\sqrt{W}} \tag{1}$$

The regression analysis of the scaled distance and peak particle velocity (ppv) values results in the forecasting equation provided below:

$$ppv = K \left(\frac{D}{\sqrt{W}} \right)^\beta \tag{2}$$

The coefficients of the equation, K and β, are named as field constants. These constants are determined by geological and technological characteristics of blast site. Within this research, 69 blast data was used for regression analysis and USBM equation is formed as:

$$ppv = 117.4 (D/\sqrt{W})^{-1.095} \tag{3}$$

Several researchers have proposed scaled-distance-based equations to predict ground vibrations [31]. The Langefors-Kihlström,

Ambraseys-Hendron and Indian Standards equations are also scaled-distance-based power-form equations. Similar to USBM equation, a correlation graph was created between SD and ppv to form Langefors-Kihlström scaled distance equation [32]. Ambraseys-Hendron equation uses cube root scaled distance [33]. Indian Standard approach uses two-thirds root scaled distance [34]. Unlike the alternative approaches, the CMRI equation maintains a linear format [35]. Formerly, Mohamadnejad et al. [36] also employed these five different empirical methods to predict ppv values and determined the site constants. All the calculated predictive equations are presented in Table 2. The coefficient of determination (R²) and the calculated Mean Absolute Error (MAE) values were also presented. USBM and Ambraseys-Hendron models perform better than the other three models. Their R² and MAE values are similar. The USBM equation is one of the most widely used and trusted equation. It is also most frequently cited attenuation equations (37, 38, 39). For this reason, USBM equation was selected as sample scaled distance-based predictor equation. In the upcoming pages, USBM equation is compared to machine learning models.

3.2 Multiple regression analysis (MRA)

Within the scope of the research, alongside the scaled distance equations, a multiple regression equation has been developed for ppv estimation [40]. The independent variables of the model are S/B, H/B and SD. Peak particle velocity is the dependent (target) variable. The resulting equation is given below:

$$ppv = (-4.993) \times S/B + (0.235) \times H/B + (-0.605) \times SD + 22.685 \tag{4}$$

Table 3 shows the regression model overview and the analysis of variance (ANOVA). The regression part of the sum of squares gives

information about the explained amount of change in the model and the dependent variable. The residual part gives information about the

unexplained amount of change in the model. The mean square is obtained by the ratio of the sum of squares value to the degrees of freedom (df) and expresses the fluctuation in the change. The ratio of

the calculated mean squares gives the F value. If the significance is less than 0.05, it can be said that there is a difference between the input and output parameters [41].

Table 2. Scaled distance-based predictor equations and calculated constants

	Scaled distance equation	Calculated constants		R ²	MAE
		K	β		
USBM	$ppv = K(\frac{D}{\sqrt{W}})^\beta$	117.4	-1.095	0.68	2.02
Langefors-Kihlström	$ppv = K(\frac{W}{D^{2/3}})^\beta$	43.09	1.2988	0.60	2.41
Ambraseys-Hendron	$ppv = K(\frac{D}{W^{1/3}})^{-\beta}$	270.86	-1.122	0.70	2.00
Indian Standard	$ppv = K(\frac{W^{2/3}}{D})^\beta$	43.09	0.9741	0.60	2.36
CMRI	$ppv = n + K(\frac{\sqrt{W}}{D})$	59.45	-	0.46	2.32

Table 3. The statistics of multiple regression model

Analysis	R	R ²	Adjusted R ²	Estimated Standard Error
1	0.716	0.513	0.490	3.99826

Independent variables: S/B, H/B, SD						
Analysis		SS	(df)	Avg. Square	F	Sig.
1	Regression	1093.741	3	364.580	22.806	0.000
	Residual	1039.094	65	15.986		
	Total	2132.835	68			

Dependent Variable: ppv
Independent Variables: S/B, H/B, SD

Sixty-nine shot data (training) were used to establish the predictive regression model. The remaining 26 blasts were separated as test data. These 69 blasts data will also be used to develop machine learning models. Using similar input parameters such as S/B, H/B, and SD, machine learning models were also developed. Figure 2 shows scatter plots of the input parameters and the peak particle velocity. The statistical values give descriptive numbers to show distribution of data. Scatter plots show the range and scattering of the data. For example, if S/B parameter is examined, it is seen that S/B value are concentrated between 1.0 and 1.3.

4. Machine Learning Prediction Models

The machine learning techniques are a form of artificial intelligence that uses specific algorithms for data analysis and development of forecasting models. In this study, ANFIS, SVM and GPR techniques were used to create prediction models. The developed models were compared to USBM and multiple regression equations. The input parameters of the machine learning models are S/B,

H/B and SD. The target of the study was to establish the most efficient models with optimum number of variables. It was avoided to create complex and difficult to use models. In the next pages, each model was described by using its own influential parameters.

4.1. Adaptive network based fuzzy inference system (ANFIS)

4.1.1. Fundamentals of ANFIS

The ANFIS method has some advantage such as capability of solving nonlinear problems, ease of use and fast computation ANFIS is a neural network rooted in the Takagi-Sugeno fuzzy system, integrating both artificial neural networks and fuzzy logic concepts. It was first developed by Jang [22]. Membership functions play a key role in Sugeno type fuzzy inference systems (FIS). It intends to specify fuzzy IF-THEN rules derived from a single output value. It combines the least squares method with backpropagation gradient descent techniques. FIS also applies a hybrid learning algorithm [42].

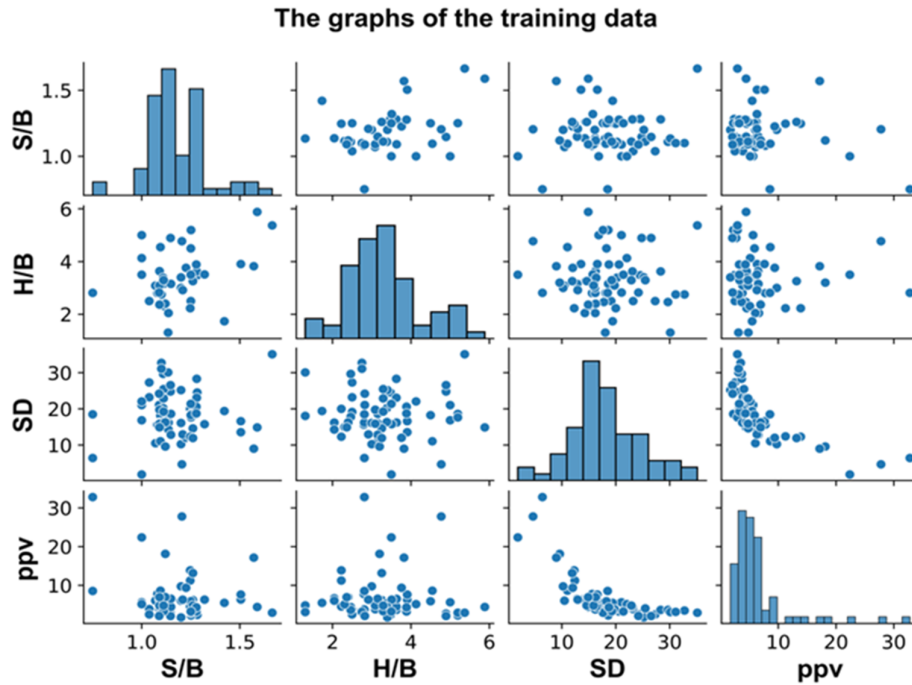


Figure 2. Scatter and histogram graphs of the model development data

ANFIS creates if-then rules using input and output information pairs. Model can define all possible rules and regulations. Also, researchers may modify considering data structure [43]. There are three types of fuzzy reasoning mechanisms: Type-1, Type-2, and Type-3. In Type-1 fuzzy inference systems, the overall output is the weighted average of the crisp outputs of each rule based on their firing strengths. The output membership functions must be monotonic [44]. In Type-2 fuzzy inference, the combined fuzzy result is derived by applying the max operation to each rule’s output, which is computed as the minimum of the firing strength and the corresponding output membership function. The final crisp output is determined using methods such as the centroid of area or the mean of maxima [45]. In Type-3 fuzzy inference, each rule follows the Takagi–Sugeno structure, where the output is expressed as a linear function of the input variables plus a constant. The final result is computed as the weighted average of the outputs from all activated rules [46]. Unlike the other types, Type-3 utilizes a linear combination of input variables along with a constant term. Therefore, it is highly appropriate for regression modeling. The model created in this study is made based on Type-3 ANFIS structure. The corresponding ANFIS framework is illustrated in Figure 3. Two fuzzy if-then rules can be described as follow:

• Rule 1: If x is A1 and y is B1, then $f_1 = p_1x + q_1y + r_1$

• Rule 2: If x is A2 and y is B2 then $f_2 = p_2x + q_2y + r_2$

Where are:

A1, A2, B1 and B2 - defined variables for inputs x and y inputs,

p_1, q_1, r_1, p_2, q_2 and r_2 - output function parameters [22].

During model development the input data is proceed through a series of layers. ANFIS equivalent architecture consists of six layers as seen in Figure 3. Static nodes are shown by circles and dynamic nodes are shown by squares [47]. The output depends on the parameters associated with the nodes. To decrease a predefined error criterion, the training rule determines how particular parameters should be modified [22].

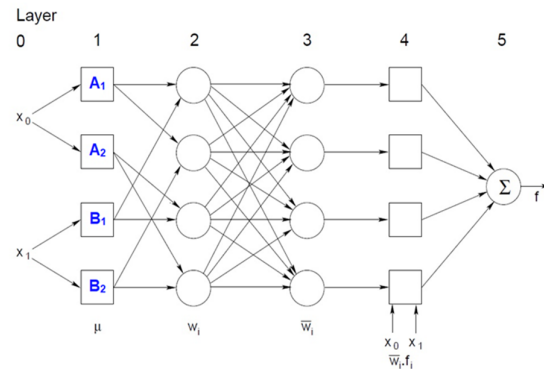


Figure 3. The fundamental structure of ANFIS and layers [48]

According to Jang [22], ANFIS consists of 6 layers and is defined as:

In Figure 3, layer 0 is the input layer. Transmitted to the subsequent layers is the input signal received from each node. Layer 1 is the fuzzification layer. Layer 2 is the multiplication layer. Each node increases the incoming data. Known as the firing strength is the output of the multiplication layer. Layer 3 is the normalization layer. To obtain an output, each rule's firing strength is divided by the total firing strength of all rules. Layer 4 is the defuzzification layer. The last operation is summation in Layer 5. To generate a comprehensive result, the sum of all incoming signals is computed [12].

4.1.2. Creating the ANFIS model

Before model development, data set is separated as training and test data. Although there are some different practices, in machine learning applications, generally 70-75% of data is separated as training data set. The remaining data (25-30%) are used as test data. Hudaverdi and Akyildiz [49] created a vibration prediction model using neural networks. They assigned 70% of the dataset for training. This ratio is also the default data splitting ratios of MATLAB software. Collazos-Escobaret al. [50] applied different machine learning techniques to control the storage conditions of dried products. 75% of data were used for model training and 25% for validation. In this study, several ratios were tested through trial-and-error process and 73% of the total data (69 sample) were separated for training data set. The training data consists of three input parameters and one output

parameter. Figure 4 presents the general structure of the ANFIS model. Following the input layer, four consecutive layers are included. These layers consist of the input membership function, the rule, the output membership function, and the output layers. The number of rules is dependent on the quantity of input membership functions [51].

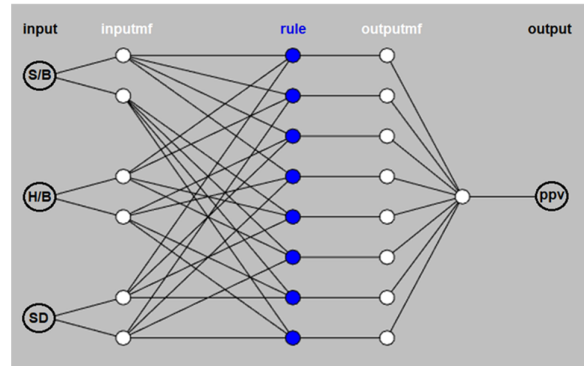


Figure 4. The suggested ANFIS structure for ppv prediction

Before starting the training process, the hybrid optimization method was chosen. The error tolerance is zero and the epoch number is 130. After identifying of the train and test data, the type and number of membership functions are selected for each input in the ANFIS interface. Based on trial-and-error process, number of membership functions was determined. Two membership functions were used for each input parameter. Totally, eight different membership functions were tested. Sigmoidal (fully symmetrical) membership function provided the lowest error value. Table 4 shows the error values of different membership functions during model development.

Table 4. Error values of membership functions

Membership function types	Matlab code	Error value
Bell-shaped Function	gbellmf	2.93418
Trapezoidal Function	trapmf	3.12354
Triangular Function	trimf	3.39081
Gaussian Function (symmetric)	gaussmf	2.9796
Gaussian Function	gauss2mf	3.10953
Pi Function	pimf	3.67426
Sigmoidal Function (symmetric)	dsigmf	1.86605
Sigmoidal Function	psigmf	1.86617

The sigmoidal membership function graphs are presented in Figure 5 for each input parameters. The model, which was created with S/B, H/B and

SD inputs includes two linguistic variables, low and high. The type of output membership function is constant.

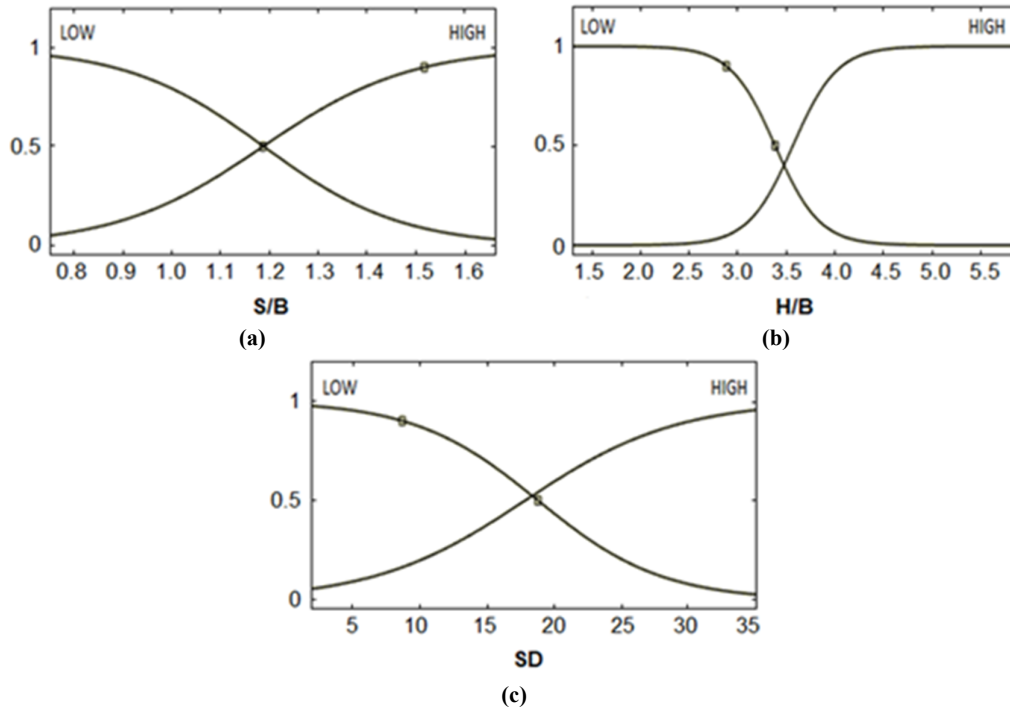


Figure 5 The assigned membership functions for a) S/B, b) H/B, and c) SD

Training performance of the ANFIS model is presented in Figure 6. In the Figure, the actual data is represented by the blue circles. The predicted values (output) by the model are shown by the red stars. The ANFIS model is quite successful. The highest prediction errors were observed For Blasts 10, 35, 58, and 61. The best estimations were achieved for the cases 2, 3, 12, 20, 32, 36, 40, 42, 51, 53 and 65.

In Figure 7, the rule diagram shows the input values and the calculated corresponding outputs, graphically. The first three columns represent the input parameters, and the last column is the output parameter, i.e., peak particle velocity. Each column marks a different rule and the figure shows all the

8 rules [52]. Additionally, the limit values of each input can be seen in this diagram. The rule diagram shows mechanism of ANFIS process. In the figure, a specific sample indicated by blue vertical lines was presented to show how the ANFIS model works. As the blue bars are moved left and right, the input values change and therefore the output results also change. S/B, H/B, and SD values are 1.21, 3.59, and 18.5, respectively, in Figure 7. The peak particle velocity (ppv) value corresponding to these values was determined as 4.28 mm/s.

Table 5 shows if-then rules for the ANFIS model. The rules in Table 5 corresponds to each row in Figure 7.

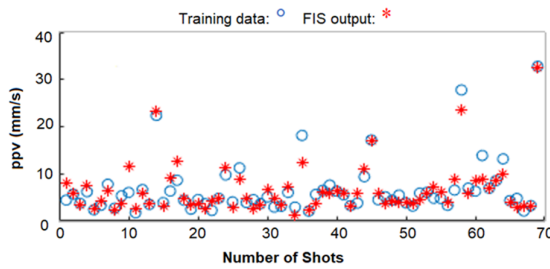


Figure 6. Actual and estimated values in the ANFIS training phase

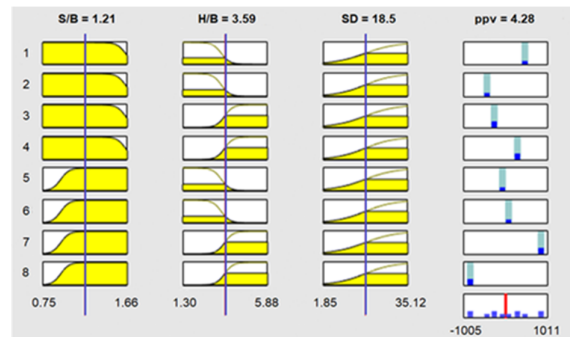


Figure 7. Rule scheme of the ANFIS model

Table 5. Fuzzy if–then rules for the proposed fuzzy model

Rule No	If-then rules
1	If (S/B is in1mf1) and (H/B is in2mf1) and (SD is in3mf1) then (output is out1mf1)
2	If (S/B is in1mf1) and (H/B is in2mf1) and (SD is in3mf2) then (output is out1mf2)
3	If (S/B is in1mf1) and (H/B is in2mf2) and (SD is in3mf1) then (output is out1mf3)
4	If (S/B is in1mf1) and (H/B is in2mf2) and (SD is in3mf2) then (output is out1mf4)
5	If (S/B is in1mf2) and (H/B is in2mf1) and (SD is in3mf1) then (output is out1mf5)
6	If (S/B is in1mf2) and (H/B is in2mf1) and (SD is in3mf2) then (output is out1mf6)
7	If (S/B is in1mf2) and (H/B is in2mf2) and (SD is in3mf1) then (output is out1mf7)
8	If (S/B is in1mf2) and (H/B is in2mf2) and (SD is in3mf2) then (output is out1mf8)

4.2. Support vector machines

4.2.1. A brief introduction to SVM

Support vector machine is a supervised learning technique grounded in statistical learning theory. For classification and regression analysis, it is a very efficient technique [23]. SVM uses a kernel function-based nonlinear mapping to convert an input space into a multidimensional space. It aims to discover a nonlinear relationship between inputs and outputs. SVM attempts to minimize the range between expected and observed values by assigning a hyperplane by reducing the coefficients, in order to provide a more efficient prediction in a regression analysis [53]. In most classification cases SVM investigates the largest separation between two classes. The larger the gap

between data sets, the better the efficiency of the SVM will be [54].

4.2.2 Creating SVM model

In the first stage, same data was used for training. Cross-validation was applied to prevent over-fitting. Cross-validation methodology splits the data into multiple groups to prevent overfitting and machine memorization [51]. Accuracy estimation is made for each divided fold. The training data can be divided into at least 2 and at most 50 clusters. In this research, all possibilities were examined by trial-and-error method to verify the data. Accordingly, the better results were obtained with 5 clusters in the cross-validation process. The common workflow of the SVM regression models is given in Figure 8.



Figure 8. Common workflow for regression models

After the selection of cross-validation methodology, the model training was started and the most efficient model (SVM Quadratic) was determined considering root mean square error (RMSE) values. The correlation coefficient was examined to determine capability of the developed SVM model. Figure 9 shows performance of the SVM model. Horizontal axis represents the measured ppv values and vertical axis represents predictions by machine learning model. The histogram graphs in Figure 9 illustrate the distribution of the predicted values corresponding actual ppv values. The measured vibration data concentrated at low ppv levels. There are few ppv data above 20 mm/s. Correspondingly, the predicted ppv values also concentrate between 2–10 mm/s. The coefficient of determination was calculated as 0.77. The results show that prediction performance for training is satisfactory and the machine works without memorization. The

calculated the mean absolute error (MAE) was 1.75 for the estimated values.

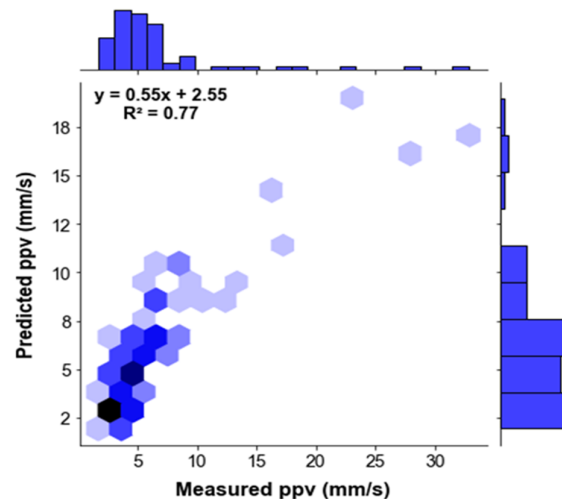


Figure 9. SVM training phase performance

4.3 Gaussian process regression (GPR)

4.3.1. Fundamentals of GPR

Gaussian process regression is non-parametric kernel-based probabilistic model and can be used for nonlinear regression analysis and data classification. GPR is a Bayesian non-parametric approach that systematically deals with

uncertainties in data [55]. A gaussian process is also characterized as a stochastic process that depends on a group of random variables [25].

The gaussian process is parameterized with an average function $m(x)$ and a covariance function (Kernel) $k(x, x')$ evaluated at points $f(x)$, x and x' . The function is defined as:

$$m(x) = E(f(x)) \tag{11}$$

$$Cov(f(x), f(x')) = k(x, x'; \theta) = E((f(x) - m(x))(f(x') - m(x')))) \tag{12}$$

Where, θ denotes the set of hyperparameters.

$$f(x) \sim GS(m(x), k(x,x')) \tag{13}$$

where GS symbolizes the gaussian process. The function $f(x)$ follows a gaussian distribution with a specified average and covariance function [25].

The covariance (kernel) function is a significant component in gaussian process regression. Similarity between data is very important in supervised learning. This similarity examination directly affects the prediction ability of models. In this study, peak particle velocity (ppv) estimation was performed using the "Exponential Covariance Function":

•Exponential covariance

$$k(X_i, X_j | \theta) = \sigma_f^2 \exp\left[-\frac{r}{\sigma_l}\right] \tag{14}$$

Where are:

$r = \sqrt{(X_i - X_j)^T (X_i - X_j)}$ - euclidian distance between X_i and X_j ,
 σ_l - the characteristic length scale,
 σ_f - the signal standard deviation.

The hyperparameters of covariance functions $\theta(\sigma_l, \sigma_f)$ can be calculated by gradient based algorithms using the equations given above.

4.3.2. Development of GPR model

During creation of gaussian process regression model, the structure of data is very important. Existence of very similar values or extreme values in dataset are the main factors that reduce performance of GPR models. Also, the test data should range between the smallest and largest values of the training data. Otherwise, the prediction model will be formed incorrectly. The common workflow of regression models given in the SVM section is also valid for Gaussian process regression.

Cross validation is applied to prevent over fitting. In the cross-validation method, the data is randomly divided into subgroups. One of the groups is used as the test set, while the others are used as the training set. Different scenarios were tried to group the data. The best results were obtained by dividing the data into 50 subgroups (folds) [56].

After selecting the validation method, the learning process starts and the best performing GPR model is determined. RMSE values are examined to evaluate the model's efficiency. Exponential covariance function provided the lowest error value. The root mean square error of the final model is around 1.86. Figure 10 shows model performance during the training stage. The prediction performance can be examined case by case for each blast.

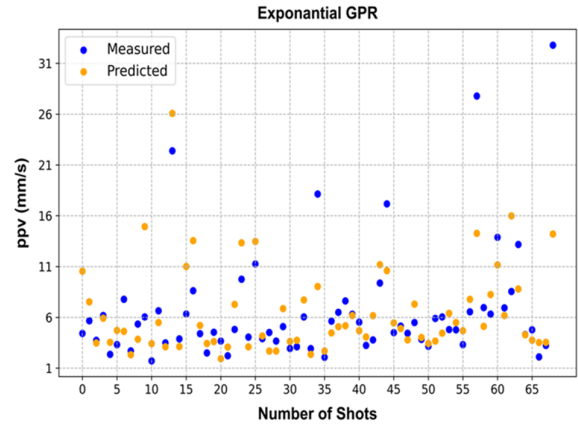


Figure 10. The forecasting efficiency of the GPR model in the training stage

5. Validation and Evaluation of Models

Various error metrics can be used to evaluate the performance of the models. Ghasemi et al. [57] evaluated the performance of their fuzzy model using the R^2 , variant for account (VAF), RMSE and mean absolute percentage error (MAPE) criteria. Srivastava et al. [53] used the R^2 metric to

demonstrate the performance of their support vector regression and random forest regression models. In addition to these criteria, this study also employed mean-based error metrics such as mean absolute error (MAE), mean absolute scaled error (MASE), and root mean square scaled error (RMSSE). Furthermore, symmetric mean absolute

percentage error (sMAPE) and the Nash–Sutcliffe Efficiency coefficient (NSE) were also considered in the evaluation. For each model, the number of blasts with a prediction error less than 2 mm/s was also determined. The formulas of all error metrics are presented in Table 6.

Table 6. Error measures for the model validation.

Error Type	Formula
Mean absolute error	$MAE = \frac{1}{n} \sum_{i=1}^n m_i - p_i $
Root mean square error	$RMSE = \sqrt{\frac{1}{n} \sum_{i=1}^n (m_i - p_i)^2}$
Mean absolute scaled error	$MASE = \frac{1}{n} \sum_{i=1}^n \frac{ m_i - p_i }{\frac{1}{n-1} \sum_{i=2}^n m_i - m_{i-1} }$
Root mean squared scale error	$RMSSE = \sqrt{\frac{1}{n} \sum_{i=1}^n \left(\frac{ m_i - p_i }{\frac{1}{n-1} \sum_{i=2}^n m_i - p_{i-1} } \right)^2}$
Mean absolute percent error	$MAPE = \frac{100}{n} \sum_{i=1}^n \frac{ m_i - p_i }{m_i}$
Symmetric mean absolute percent error	$sMAPE = \frac{200}{n} \sum_{i=1}^n \frac{ m_i - p_i }{m_i + p_i}$
Variance account for	$VAF = \left(1 - \frac{var(m_i - p_i)}{var m_i} \right) * 100$
Nash-Sutcliffe efficiency	$NSE = 1 - \frac{\sum_i^n (m_i - p_i)^2}{\sum_i^n (m_i - \bar{m}_i)^2}$

m_i = measured particle velocity (mm/s); p_i = predicted particle velocity (mm/s); n = case number

Table 7 shows comparison of the created models according to the introduced error criteria. MAE is 1.42 for ANFIS model. The calculated MAE values are 1.82 and 1.46 for SVM and GPR models, respectively (Table 6). RMSSE values are under 0.50 for ANFIS and GPR models. The lowest MAPE values were obtained by ANFIS and GPR models. SVM model has the third lowest MAE value. The RMSE and RMSSE values calculated for the SVM model are 2.57 and 0.51, respectively.

Twenty-one blasts were predicted with an error of lower than 2 mm/s by GPR. The multiple regression equation estimated only 13 cases with an error of less than 2 mm/s. In general, Machine learning models have lower error values than scaled-distance-based USBM equation and multiple regression equation. The most successful results were obtained for ANFIS model.

Table 7. Calculated error values for the vibration prediction models

	MAE	RMSE	MASE	RMSSE	MAPE	sMAPE	VAF	NSE	< 2 mm/s
ANFIS	1.42	1.84	0.28	0.37	22.30	19.70	90.18	0.89	20
SVM	1.82	2.57	0.36	0.51	30.03	24.44	79.27	0.79	18
GPR	1.46	2.29	0.29	0.45	23.29	20.29	83.90	0.84	21
USBM	2.03	2.97	0.41	0.59	23.33	23.21	74.88	0.72	17
MRA	2.32	2.94	0.46	0.59	38.09	151.16	74.08	0.73	13

The correlation graphs of the models are given in Figure 11. The R^2 is 0.9 for ANFIS model. The correlation graph of GPR model also indicates high prediction performance. The lowest R^2 value was obtained by multiple regression equation (Figure 11). It should be noted that the correlation between

the estimated and measured values for all models is quite high. R^2 value of 0.65 corresponds to 80% correlation. The correlation between the observed and estimated values was also analyzed for the USBM equation. The calculated R^2 value for USBM equation is around 0.75.

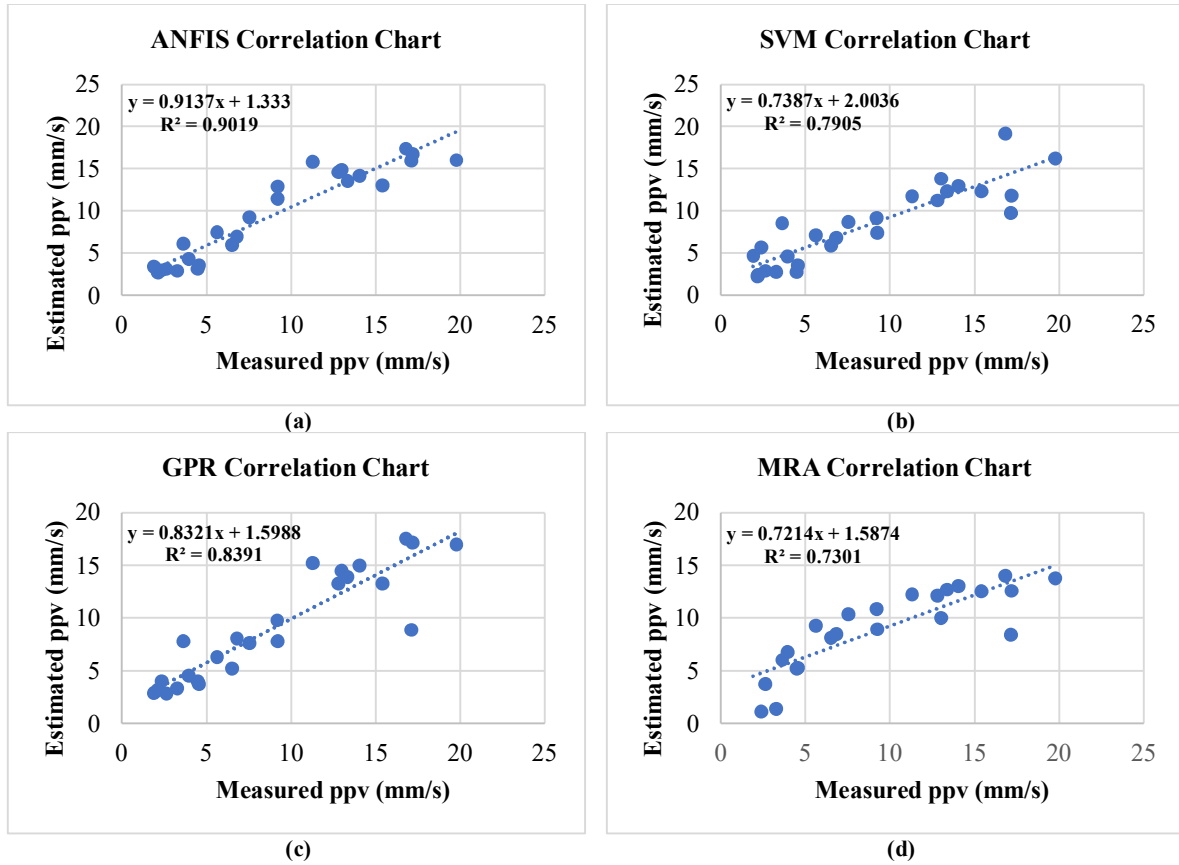


Figure 11. Correlation charts of the prediction models

Figure 12 illustrates a radar graph. The numerical ranges of the error metrics are different. Only the error metrics with similar value ranges were selected to make a radar graph. By that way, a specific radar graph was created. Figure 12 shows radar graph of the mean error metrics. A small tetragon means low prediction error. USBM equation has the largest tetragon shape. All machine learning tetragons are inside USBM tetragon. That indicates superiority of the machine learning models. Relatively the most successful model is ANFIS. GPR is the second most efficient model.

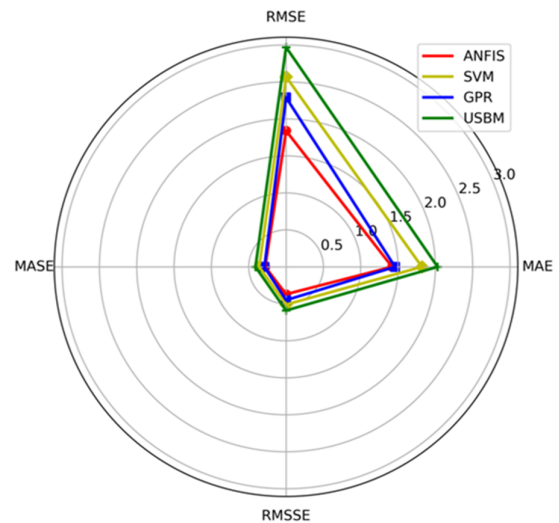


Figure 12. A radar graph based on mean error criteria

6. Conclusions

In this study, blast-induced ground vibration was estimated using a database obtained from a quarry in Istanbul Kemerburgaz Region. Since quarries are close to settlements, environmental impacts become more important. Vibration data were measured by blast seismographs and handheld GPS devices were used for distance measurements. In the first step, scaled distance equations were created for ground vibration estimation. Six scaled-distance-based equations were examined considering the coefficient of determinations. the USBM equation was chosen to compare with the machine learning models.

In the second stage, a multiple regression equation and three different machine learning methods (ANFIS, SVM, GPR) were developed. Stiffness ratio, energy coverage and scaled distance were used as input parameters. A rigorous model validation was achieved. In general, the machine learning techniques are found to be more effective than traditional regression models. ML methods predicted 18-21 cases with an error less than 2 mm/s. The VAF values obtained for the ML models are over 79%. The ANFIS model provided the best results for 8 out of 9 error criteria. The GPR model has the second lowest error values. There is a strong relationship between the observed and estimated ppv values. The coefficient of determination (R^2) is higher than 0.90 for ANFIS model. The R^2 values for the GPR and SVM models are 0.84 and 0.79, respectively.

In this research, it was concluded that some specific parameters are important for success of the ML models. In the ANFIS modeling technique, influential factors are the type of input and output membership functions, the number of rules, and the number of subgroups for input parameters. Selection of the appropriate covariance (Kernel) function, cross-validation method and clustering number play an important role in the success of GPR model. The verification method and the number of subgroups (clustering) directly affect the performance of SVM. The main difference between GPR and SVM models are their prediction methodology during model training phase.

Blasting operation is a complex process and affected by several parameters. It has been proven that machine learning methods can be used successfully to predict particle velocity. Machine learning methods are flexible and adaptive techniques. In the future, it is possible to renew the models by using different databases and different input parameters. Machine learning and artificial

intelligence will help to forecast blast vibrations more accurately.

References

- [1]. Jimeno, C. L., Jimeno, E. L., Carcedo, F. J. A., & de Ramiro, Y. V. (1995). Drilling and blasting of rocks. *USA CRS Press*, 41, 35947.
- [2]. Konya, C. J., & Walter, E. J. (1990). Surface blast design. (*No Title*).
- [3]. Mansouri, H., & EBRAHIMI, F. M. (2015). Blast vibration modeling using linear superposition method.
- [4]. Kahriman, A. (2004). Analysis of parameters of ground vibration produced from bench blasting at a limestone quarry. *Soil Dynamics and Earthquake Engineering*, 24(11), 887-892.
- [5]. Ataei, M. (2010). Evaluation of blast induced ground vibrations from underground excavation at Karoun 3 area. *Mining Technology*, 119(1), 7-13.
- [6]. Yilmaz, O. (2016). The comparison of most widely used ground vibration predictor equations and suggestions for the new attenuation formulas. *Environmental earth sciences*, 75(3), 269.
- [7]. Hudaverdi, T., & Akyildiz, O. (2019). Evaluation of capability of blast-induced ground vibration predictors considering measurement distance and different error measures. *Environmental Earth Sciences*, 78(14), 421.
- [8]. Soltani-Mohammadi, S., Amnieh, H. B., & Bahadori, M. (2011). Predicting ground vibration caused by blasting operations in Sarcheshmeh copper mine considering the charge type by Adaptive Neuro-Fuzzy Inference System (ANFIS). *Archives of Mining Sciences*, 56(4), 701-710.
- [9]. Kamali, M., & Ataei, M. (2010). Prediction of blast induced ground vibrations in Karoun III power plant and dam: a neural network. *Journal of the Southern African Institute of Mining and Metallurgy*, 110(8), 481-490.
- [10]. Kamali, M., & Ataei, M. (2011). Prediction of blast induced vibrations in the structures of Karoun III power plant and dam. *Journal of Vibration and Control*, 17(4), 541-548.
- [11]. Armaghani, D. J., Momeni, E., Abad, S. V. A. N. K., & Khandelwal, M. (2015). Feasibility of ANFIS model for prediction of ground vibrations resulting from quarry blasting. *Environmental earth sciences*, 74, 2845-2860.
- [12]. Akyildiz, O., & Hudaverdi, T. (2020). ANFIS modelling for blast fragmentation and blast-induced vibrations considering stiffness ratio. *Arabian Journal of Geosciences*, 13(21), 1162.
- [13]. Hasanipanah, M., Monjezi, M., Shahnazar, A., Armaghani, D. J., & Farazmand, A. (2015). Feasibility of indirect determination of blast induced ground

vibration based on support vector machine. *Measurement*, 75, 289-297.

[14]. Dindarloo, S. R. (2015). Peak particle velocity prediction using support vector machines: a surface blasting case study. *Journal of the Southern African Institute of Mining and Metallurgy*, 115(7), 637-643.

[15]. Monjezi, M., Baghestani, M., Shirani Faradonbeh, R., Pourghasemi Saghand, M., & Jahed Armaghani, D. (2016). Modification and prediction of blast-induced ground vibrations based on both empirical and computational techniques. *Engineering with Computers*, 32, 717-728.

[16]. Faradonbeh, R. S., & Monjezi, M. (2017). Prediction and minimization of blast-induced ground vibration using two robust meta-heuristic algorithms. *Engineering with Computers*, 33, 835-851.

[17]. Ataei, M., & Sereshki, F. (2017). Improved prediction of blast-induced vibrations in limestone mines using Genetic Algorithm. *Journal of Mining and Environment*, 8(2), 291-304.

[18]. Mohammadi, D., Mikaeil, R., & Abdollahei Sharif, J. (2020). Investigating and ranking blasting patterns to reduce ground vibration using soft computing approaches and MCDM technique. *Journal of Mining and Environment*, 11(3), 881-897.

[19]. Komadja, G. C., Rana, A., Glodji, L. A., Anye, V., Jadaun, G., Onwualu, P. A., & Sawmliana, C. (2022). Assessing ground vibration caused by rock blasting in surface mines using machine-learning approaches: A comparison of CART, SVR and MARS. *Sustainability*, 14(17), 11060.

[20]. Nguyen, H., Bui, X. N., & Topal, E. (2023). Enhancing predictions of blast-induced ground vibration in open-pit mines: Comparing swarm-based optimization algorithms to optimize self-organizing neural networks. *International Journal of Coal Geology*, 275, 104294.

[21]. Chandrahas, N. S., Choudhary, B. S., Teja, M. V., Venkataramayya, M. S., & Prasad, N. K. (2022). XG boost algorithm to simultaneous prediction of rock fragmentation and induced ground vibration using unique blast data. *Applied Sciences*, 12(10), 5269.

[22]. Jang, J. S. (1993). ANFIS: adaptive-network-based fuzzy inference system. *IEEE transactions on systems, man, and cybernetics*, 23(3), 665-685.

[23]. Vapnik, V. (1998). Statistical learning theory. *John Wiley & Sons google schola*, 2, 831-842.

[24]. Schiilkop, P. B., Burgest, C., & Vapnik, V. (1995, August). Extracting support data for a given task. In *Proceedings, First International Conference on Knowledge Discovery & Data Mining. AAAI Press, Menlo Park, CA* (pp. 252-257).

[25]. Williams, C. K., & Rasmussen, C. E. (2006). *Gaussian processes for machine learning* (Vol. 2, No. 3, p. 4). Cambridge, MA: MIT press.

[26]. Olofsson, S. O. (1990). Applied explosives technology for construction and mining. (*No Title*).

[27]. Hudaverdi, T., & Akyildiz, O. (2021). An alternative approach to predict human response to blast induced ground vibration. *Earthquake engineering and engineering vibration*, 20, 257-273.

[28]. Özgül, N. (2012). Stratigraphy and some structural features of the Istanbul Paleozoic. *Turkish Journal of Earth Sciences*, 21(6), 817-866.

[29]. Basu, D., & Sen, M. (2005, July). Blast induced ground vibration norms—a critical review. In *National Seminar on Policies, Statutes & Legislation in Mines* (pp. 112-113).

[30]. Duvall, W. I., & Petkof, B. (1959). *Spherical propagation of explosion-generated strain pulses in rock* (No. 5481-5485). US Department of the Interior, Bureau of Mines.

[31]. Dao, H., Pham, T. L., & Hung, N. P. (2021). Study on an online vibration measurement system for seismic waves caused by blasting for mining in Vietnam. *Journal of Mining and Environment*, 12(2), 313-325.

[32]. Langefors, U., & Kihlström, B. (1963). The modern technique of rock blasting. (*No Title*).

[33]. Stagg, K. G., & Zienkiewicz, O. C. (1968). Rock mechanics in engineering practice. (*No Title*).

[34]. Standard, I. (1973). Criteria for Safety and Design of Structures Subjected to Underground Blast, ISI. *IS-6922*.

[35]. Roy, P. P. (1993). Putting ground vibration predictions into practice. *Colliery Guardian;(United Kingdom)*, 241(2).

[36]. Mohamadnejad, M., Gholami, R., & Ataei, M. (2012). Comparison of intelligence science techniques and empirical methods for prediction of blasting vibrations. *Tunnelling and Underground Space Technology*, 28, 238-244.

[37]. Ataei, M., & Kamali, M. (2013). Prediction of blast-induced vibration by adaptive neuro-fuzzy inference system in Karoun 3 power plant and dam. *Journal of Vibration and Control*, 19(12), 1906-1914.

[38]. Agrawal, H., & Mishra, A. K. (2019). Modified scaled distance regression analysis approach for prediction of blast-induced ground vibration in multi-hole blasting. *Journal of Rock Mechanics and Geotechnical Engineering*, 11(1), 202-207.

[39]. Khan, M. F. H., Hossain, M. J., Ahmed, M. T., Monir, M. U., Rahman, M. A., Sweety, T. S., ... & Shovon, S. M. (2025). Ground vibration effect evaluation due to blasting operations. *Heliyon*, 11(2).

- [40]. IBM Corporation. (2016). *IBM SPSS Statistics Base 24*. Armonk, NY: IBM Corporation.
- [41]. Kalaycı, Ş. (2010). *SPSS uygulamalı çok değişkenli istatistik teknikleri* (Vol. 5, p. 359). Ankara, Turkey: Asil Yayın Dağıtım.
- [42]. OLIVER. NELLES. (2020). *NONLINEAR SYSTEM IDENTIFICATION: From Classical Approaches to Neural Networks, Fuzzy Systems,... and Gaussian Processes*. SPRINGER NATURE.
- [43]. Özkan, İ., Ciniviz, M., & Candan, F. (2015). Estimating Engine Performance and Emission Values Using ANFIS/ANFIS Kullanılarak Motor Performans ve Emisyon Değerleri Tahmini. *International Journal of Automotive Engineering and Technologies*, 4(1), 63-67.
- [44]. Tsukamoto, Y. (1979). An approach to fuzzy reasoning method. *Advances in fuzzy set theory and applications*.
- [45]. Lee, C. C. (1990). Fuzzy logic in control systems: fuzzy logic controller. I. *IEEE Transactions on systems, man, and cybernetics*, 20(2), 404-418.
- [46]. Takagi, T., & Sugeno, M. (1983). Derivation of fuzzy control rules from human operator's control actions. *IFAC proceedings volumes*, 16(13), 55-60.
- [47]. Yılmaz, M., Çomaklı, Ö., & Haşiloğlu, A. S. (2002). Kanallarda zamana bağlı zorlanmış ısı taşınımının bulanık-sinir ağı (neuro-fuzzy) ile tahmini. *GAP IV. Mühendislik Kongresi Bildiriler Kitabı*, 06-08.
- [48]. Şişman, Y., & Arzu, A. (2003). *A temporal neuro-fuzzy approach for time series analysis* (Doctoral dissertation, Middle East Technical University, Department of Computer Engineering). Ankara, Türkiye
- [49]. Hudaverdi, T., & Akyıldız, O. (2021). Prediction and evaluation of blast-induced ground vibrations for structural damage and human response. *Arabian Journal of Geosciences*, 14(5), 378.
- [50]. Collazos-Escobar, G. A., Gutiérrez-Guzmán, N., Váquiro, H. A., García-Pérez, J. V., & Cárcel, J. A. (2025). Analysis of Machine Learning Algorithms for the Computer Simulation of Moisture Sorption Isotherms of Coffee Beans. *Food and Bioprocess Technology*, 1-12.
- [51]. Works, M. (2017). Statistics and machine learning Toolbox user's guide. *Matwork Inc*.
- [52]. Hudaverdi, T. (2022). Prediction of flyrock throw distance in quarries by variable selection procedures and ANFIS modelling technique. *Environmental Earth Sciences*, 81(10), 281.
- [53]. Srivastava, A., Choudhary, B. S., & Sharma, M. (2021). A comparative study of machine learning methods for prediction of blast-induced ground vibration. *Journal of Mining and Environment*, 12(3), 667-677.
- [54]. Molavi Nojumi, M., Huang, Y., Hashemian, L., & Bayat, A. (2022). Application of machine learning for temperature prediction in a test road in Alberta. *International Journal of Pavement Research and Technology*, 15(2), 303-319.
- [55]. Arthur, C. K., Temeng, V. A., & Ziggah, Y. Y. (2020). Novel approach to predicting blast-induced ground vibration using Gaussian process regression. *Engineering with Computers*, 36(1), 29-42.
- [56]. MathWorks. (n.d.). *Support vector machine regression*. Retrieved February 10, 2022, from <https://www.mathworks.com/help/stats/support-vector-machine-regression.html>
- [57]. Ghasemi, E., Ataei, M., & Hashemolhosseini, H. (2013). Development of a fuzzy model for predicting ground vibration caused by rock blasting in surface mining. *Journal of Vibration and Control*, 19(5), 755-770.



دانشگاه صنعتی شاهرود

نشریه مهندسی معدن و محیط زیست

www.jme.shahroodut.ac.ir نشانی نشریه:



انجمن مهندسی معدن ایران

کاربرد الگوریتم‌های یادگیری ماشین برای پیش‌بینی ارتعاش زمین ناشی از انفجار از نظر نسبت سختی، پوشش انرژی و فاصله مقیاس شده

یاشار آگان^{*}، و تور کر هوداوردی

دانشکده مهندسی معدن، دانشگاه فنی استانبول، استانبول، ترکیه

چکیده	اطلاعات مقاله
<p>هدف از این تحقیق، پیش‌بینی ارتعاش زمین ناشی از انفجار در معادن سطحی با استفاده از الگوریتم‌های یادگیری کلاسیک و ماشینی است. به منظور به حداقل رساندن ارتعاش زمین ناشی از انفجار به سطوح قابل قبول، سطح ارتعاش باید پیش‌بینی شود. ارتعاش زمین ناشی از انفجار، سرعت اوج ذرات (ppv) در زمین تعریف می‌شود. تمام داده‌های مورد استفاده برای تخمین با مشاهده عملیات انفجار واقعی به دست آمده‌اند. پس از اندازه‌گیری سرعت اوج ذرات، مدل‌های پیش‌بینی با استفاده از پارامترهای مستقل سایت ایجاد شدند. بیشتر داده‌ها برای آموزش مدل استفاده می‌شوند، در حالی که بخش باقی مانده برای آزمایش استفاده می‌شود. مدل‌ها به طور متناسب با استفاده از پارامترهای مستقل انفجار ایجاد شدند. بنابراین، پارامترهای بیشتری بدون پیچیده کردن مدل‌ها در مدل‌ها گنجانده شده‌اند. یک فرآیند اعتبارسنجی کامل با استفاده از مجموعه‌ای متنوع از نه معیار خطا انجام شد. مشخص شده است که مدل‌های هوش مصنوعی در پیش‌بینی ارتعاش زمین از روش‌های سنتی بهتر عمل می‌کنند. میانگین مقادیر خطای مطلق برای ANFIS، GPR و SVM به ترتیب ۱.۴۲، ۱.۵۴ و ۱.۷۸ بود. وضعیت مشابهی برای سایر معیارهای خطا نیز مشاهده می‌شود. به نظر می‌رسد ANFIS مؤثرترین مدل برای پیش‌بینی ارتعاش زمین باشد.</p>	<p>تاریخ ارسال: ۲۰۲۵/۰۱/۳۱ تاریخ داوری: ۲۰۲۵/۰۴/۲۲ تاریخ پذیرش: ۲۰۲۵/۰۵/۱۶</p> <p><i>DOI: 10.22044/jme.2025.15686.3016</i></p> <p>کلمات کلیدی سیستم استنتاج فازی مبتنی بر شبکه تطبیقی (ANFIS) انفجار رگرسیون فرآیند گاوسی (GPR) ارتعاش زمین ماشین بردار پشتیبان (SVM)</p>